Biocompatible hydrogel as a Template for Oxidative Decomposition Reaction: A Chemodosimetric Analysis and In-Vitro Imaging of Hypochlorite

Dipen Biswakarma,[a] Nilanjan Dey [a] and Santanu Bhattacharya *[a,b,c]

[a]Department of Organic Chemistry, Indian Institute of Science, Bangalore, Karnataka 560012, India

[b]School of Applied & Interdisciplinary Sciences, Indian Association for the Cultivation of Science, Jadavpur, Kolkata 700 032, India

Email: sb@iisc.ac.in

[c]Jawaharlal Nehru Centre for Advanced Scientific Research, Jakkur, Bengaluru 560064, Karnataka, India

Synthetic Scheme:

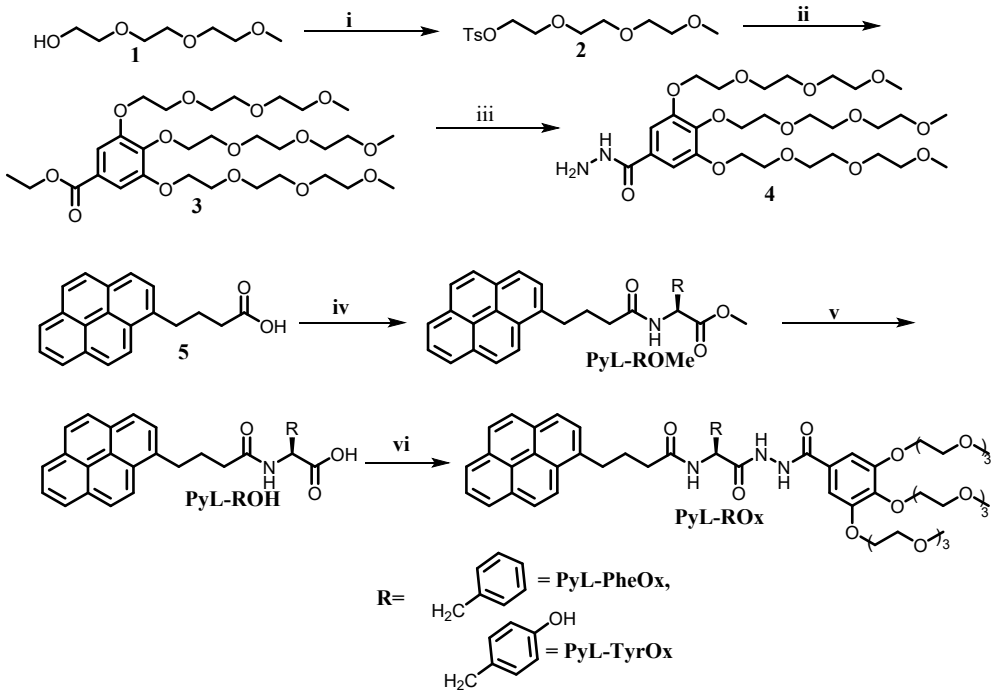

Reagents, conditions, and yields: i) NaOH, H_2O, TsCl, 6h, rt, 98%; ii) Ethyl gallate, K_2CO_3, DMF, 80 °C, 48 h, 75%; iii) $NH_2NH_2.H_2O$, MeOH, 65 °C, 24h, 96%; iv) L-amino acid methyl ester. HCl, DCC, HOBt, DCM, 0 °C- rt, 24 h, 85%; v) MeOH, 1M NaOH, 10 h, rt, 95 %; vi) **4**, DCC, HOBt, DCM, 0 °C- rt, 24h, 78%.

Synthesis: Synthesis of **4** and **PyL-PheOx** was carried out according to reported procedure. S1a-b

Synthesis of PyL-TyrOH: **PyL-TyrOMe** (2 g, 4.29 mmol) was at first dissolved in MeOH and 1M NaOH (7 mL) was added to it. The resultant mixture was stirred, and the reaction progress was monitored using thin layer chromatography (TLC). After 12 h reaction mixture was removed, and the methanol was evaporated using vacuum. The resultant residue was then taken in 40 mL water followed by washing using diethyl ether twice. The pH of an aqueous solution was also adjusted to 2.0 by adding 1M HCl. The aqueous layer so obtained was extracted using ethyl acetate. The solvent was evaporated using vacuum to give off white solid product. 91.6 % yield. m.p.186 °C, IR (Neat, cm^{-1}) 3450, 3421, 3323, 3064, 2678, 1704, 1648, 1606, 1405, 1220, 1177, 1012; ^1H NMR (400 MHz, DMSO-d_6) δ 1.92-1.98 (m, 2H), 2.22-2.26 (m, 2H), 2.72-2.78 (m, 1H), 2.94-2.99 (m, 1H), 3.22-3.26 (m, 2H), 4.38-4.43 (m, 1H), 6.64-6.66 (d, J = 8.4 Hz, 1H), 7.04-7.06 (d, J = 8 Hz, 2H), 7.88-7.90 (d, J = 8.0 Hz, 1H), 8.04-8.08 (m, 1H), 8.11-8.18 (m, 2H), 8.20-8.22 (m, 2H), 8.26-8.29 (m, 2H), 8.33-8.36 (m, 1H), 9.19 (s, 1H) ; HRMS: m/z calcd. for $C_{29}H_{25}NO_4$ $(M + H)^+$: 474.1681, found: 474.1683.

ESI-MS of **PyL-PheOx**

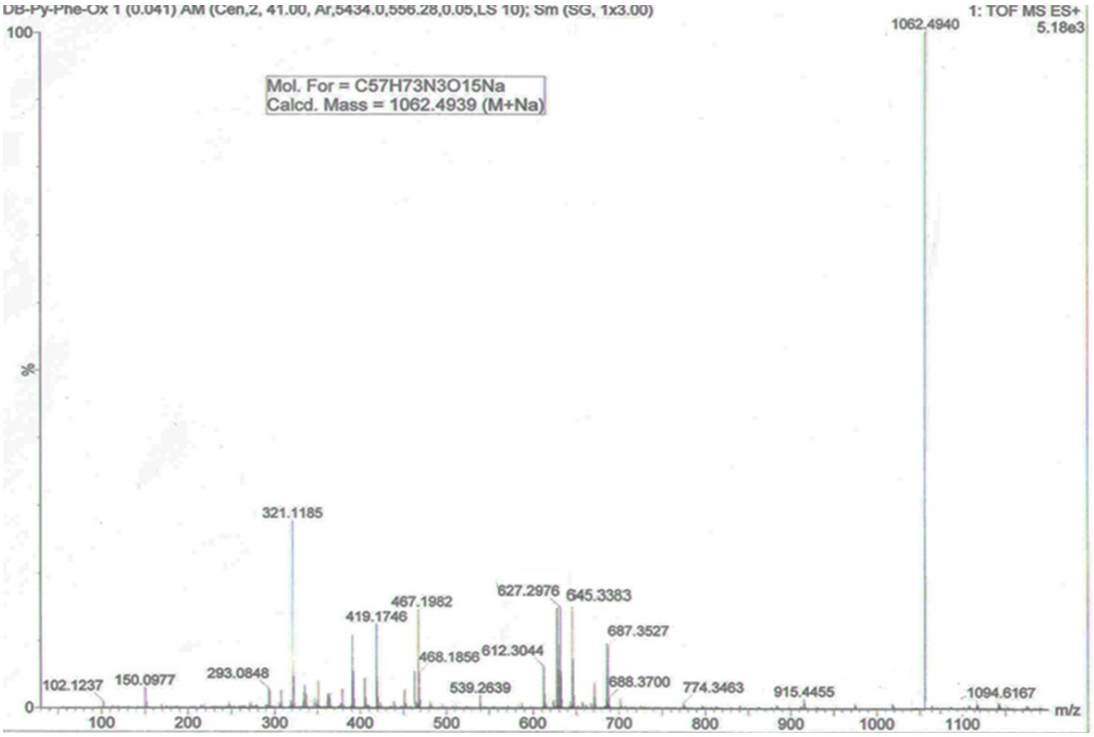

^{1}H NMR of **PyL-PheOx**

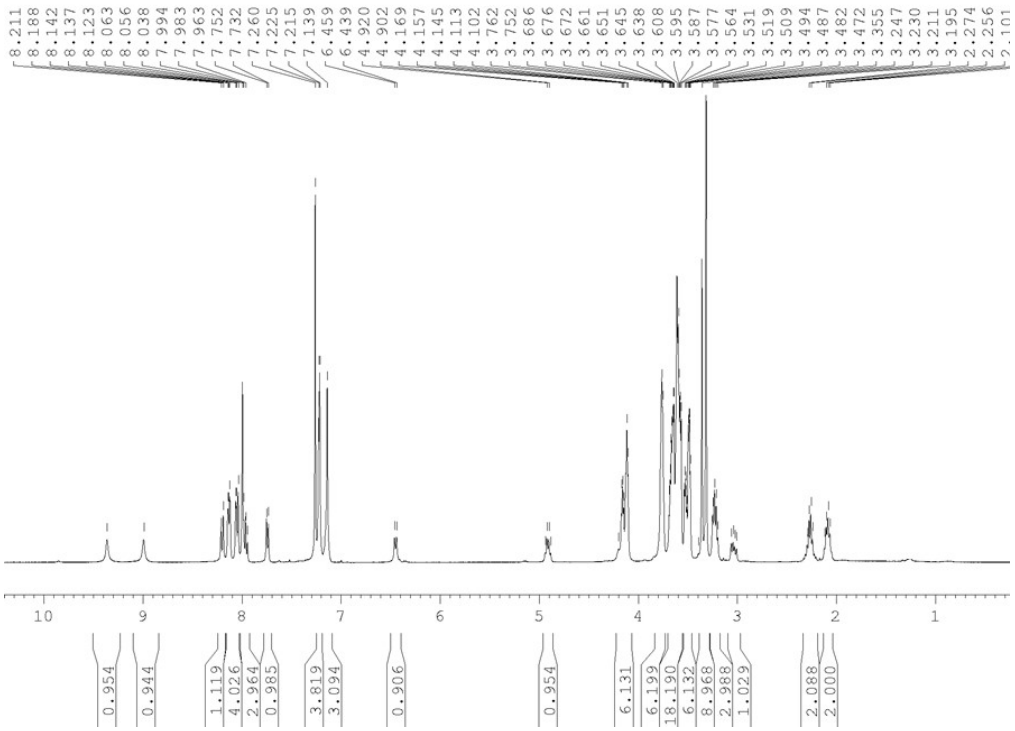

^{13}C NMR of **PyL-PheOx**

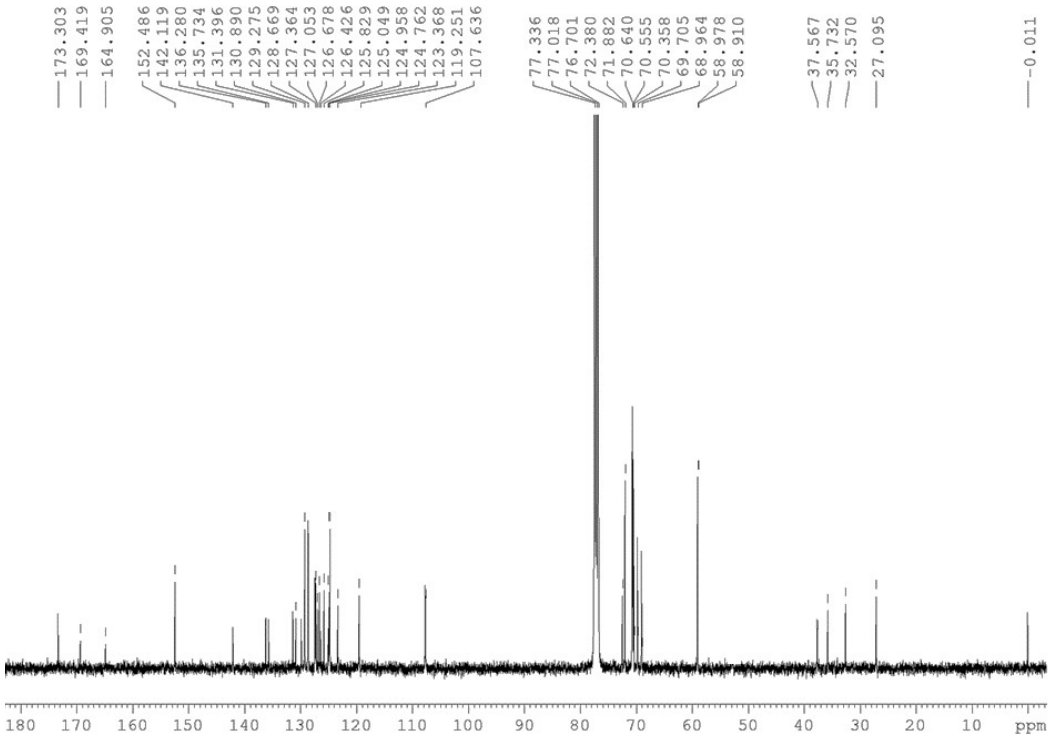

ESI-Mass of **PyL-TyrOx**

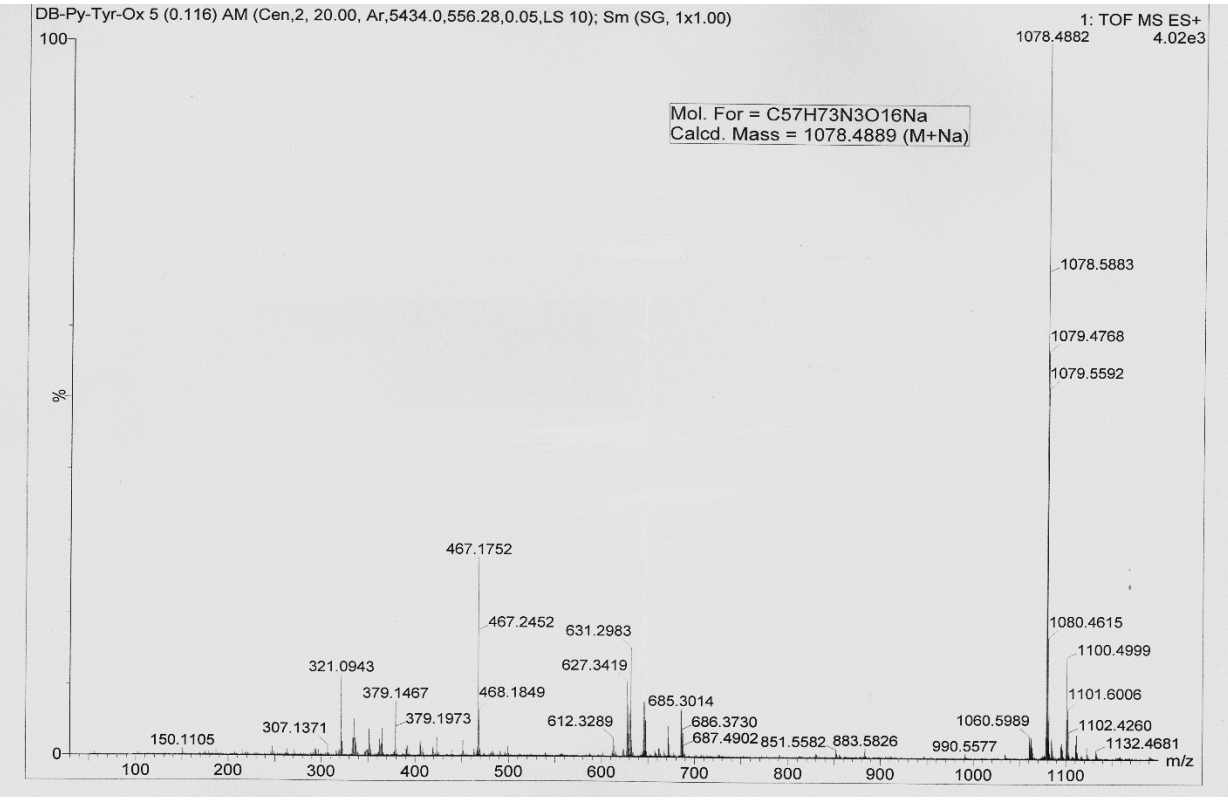

^{1}H NMR of **PyL-TyrOx**

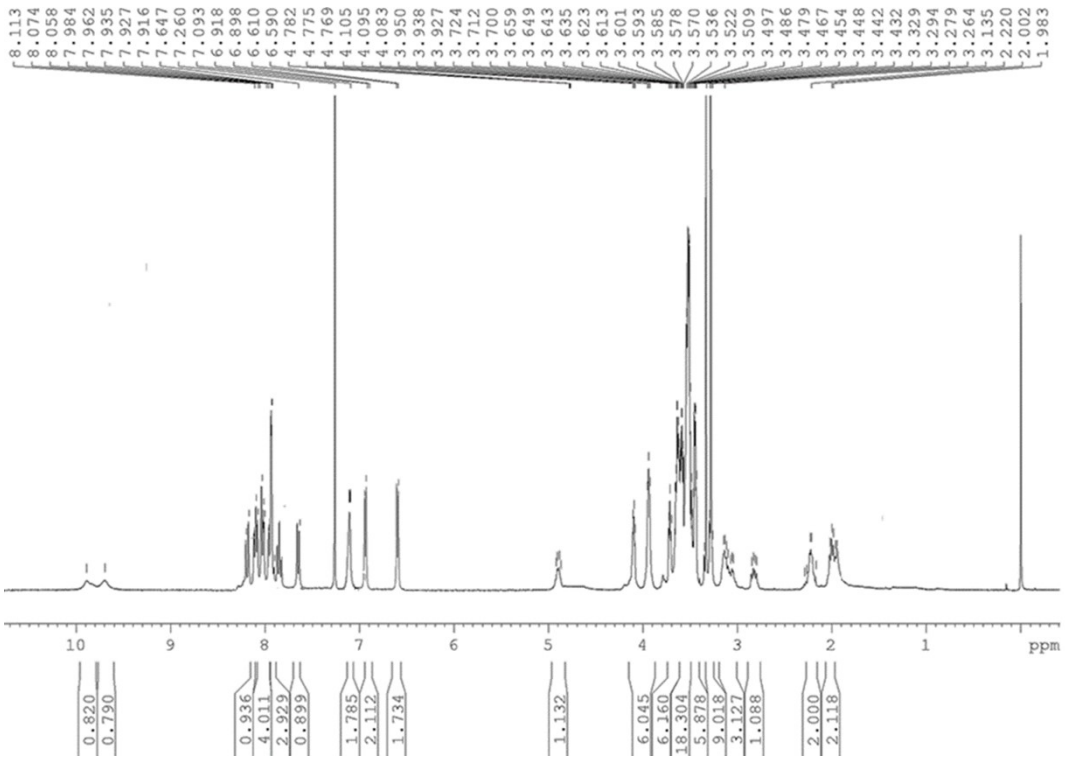

^{13}C NMR of **PyL-TyrOx**

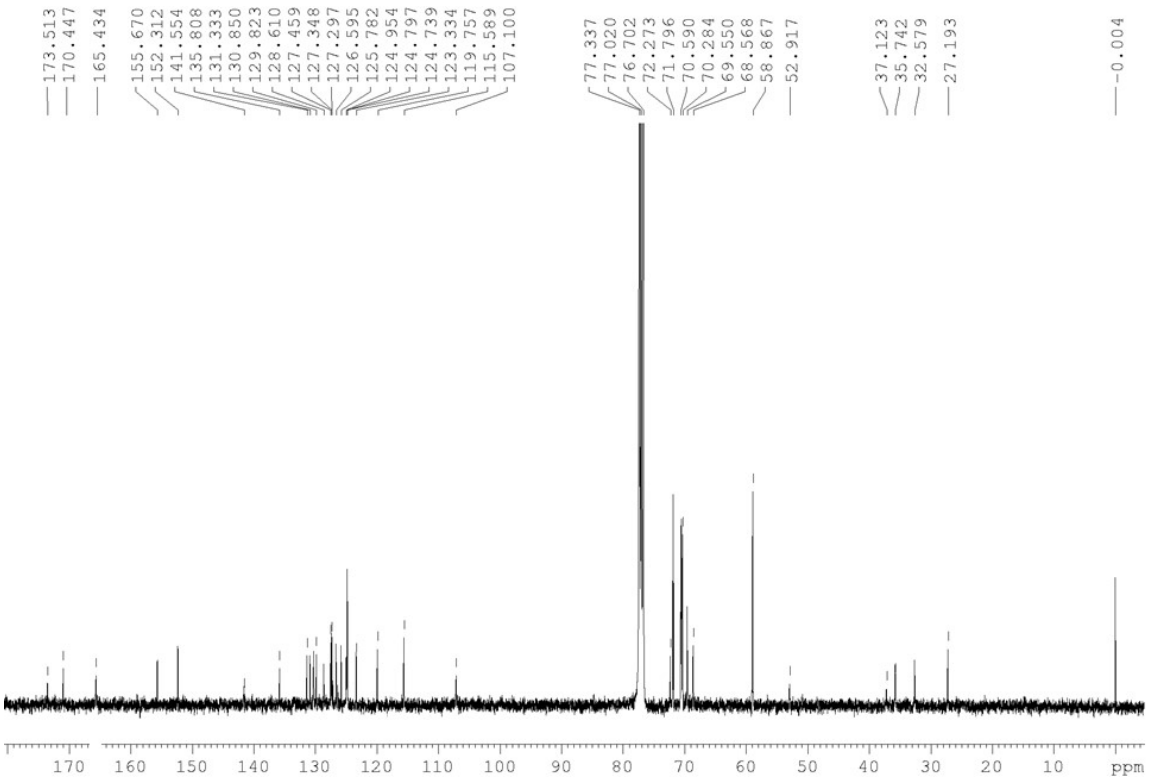

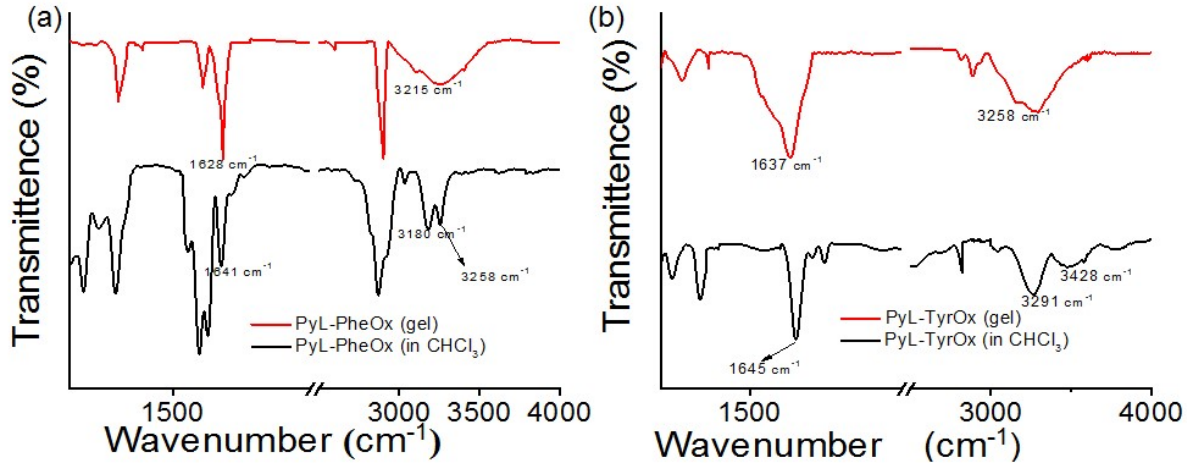

Figure S1. FT-IR spectra of (a) **PyL-PheOx** and (b) **PyL-TyrOx** in gel state and $CHCl_3$.

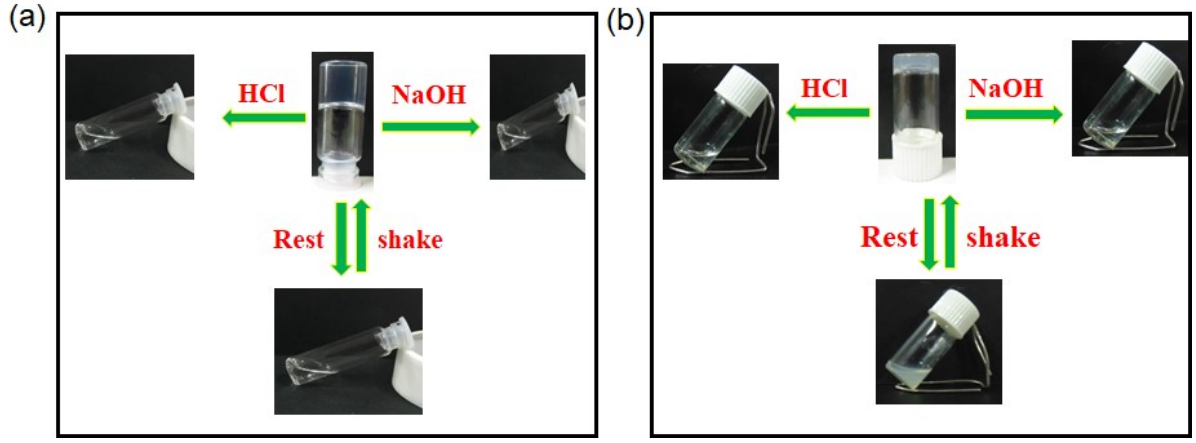

Figure S2. Gel-to-sol transition of (a) **PyL-PheOx** and (b) **PyL-TyrOx** in the presence of pH and Shake/Rest.

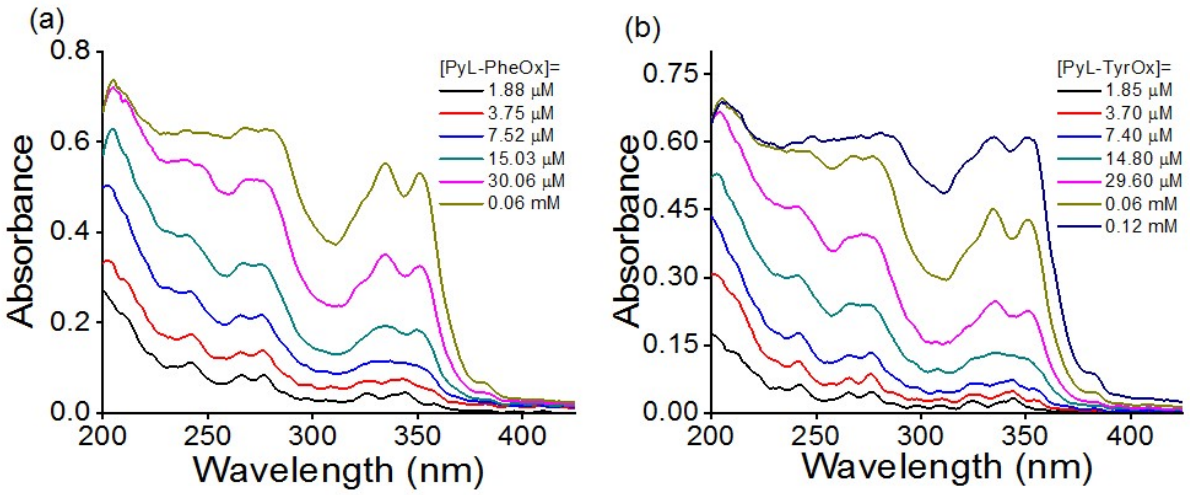

Figure S3. Concentration dependent UV-Vis's spectra of (a) **PyL-PheOx** and (b) **PyL-TyrOx** in water.

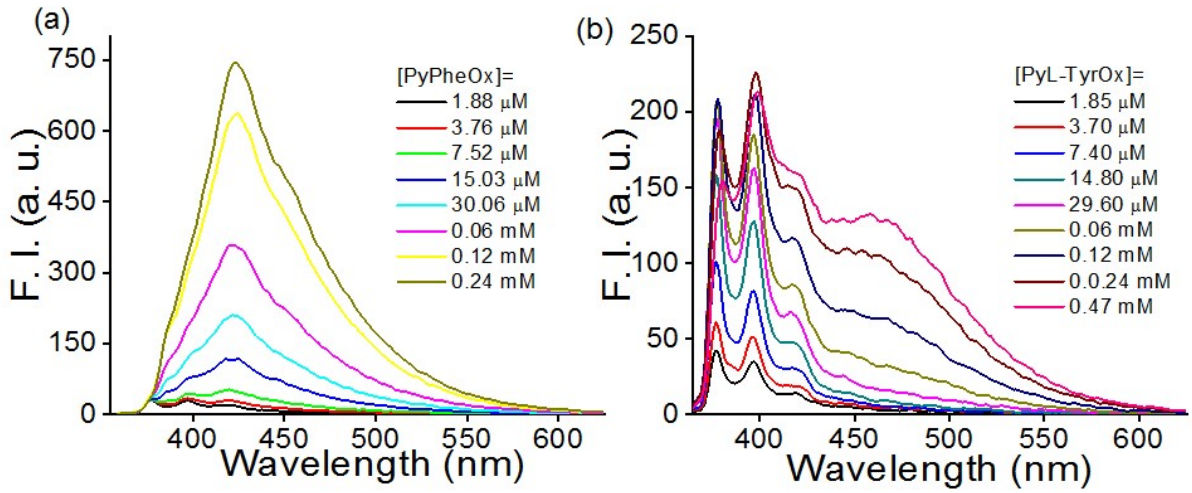

Figure S4. Concentration dependent fluorescence spectra of (a) **PyL-PheOx** and (b) **PyL-TyrOx** in water (λ_{ex} = 345 nm).

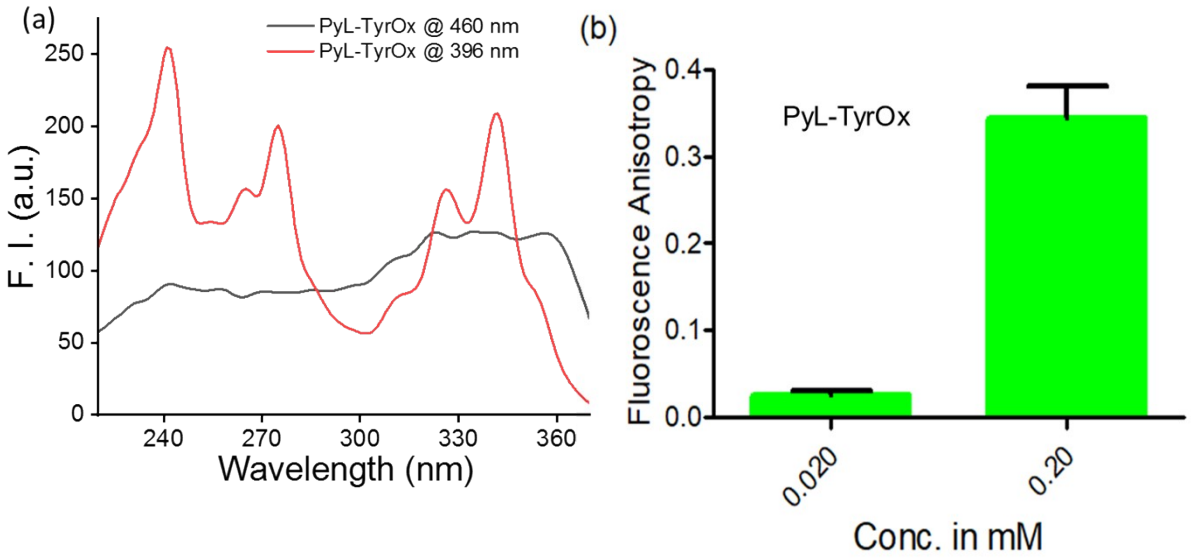

Figure S5. (a) Excitation spectra of **PyL-TyrOx** in water. (b) Fluorescence anisotropy of **PyL-TyrOx** at two different concentrations at 460 nm.

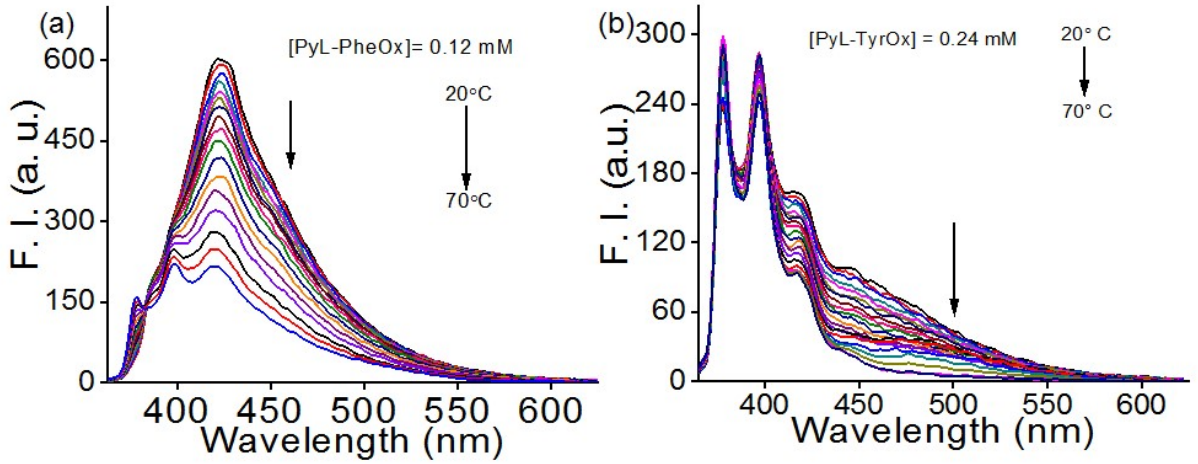

Figure S6. Variable temperature fluorescence spectra of (a) **PyL-PheOx** (0.12 mM) and (b) **PyL-TyrOx** (0.24 mM) in water.

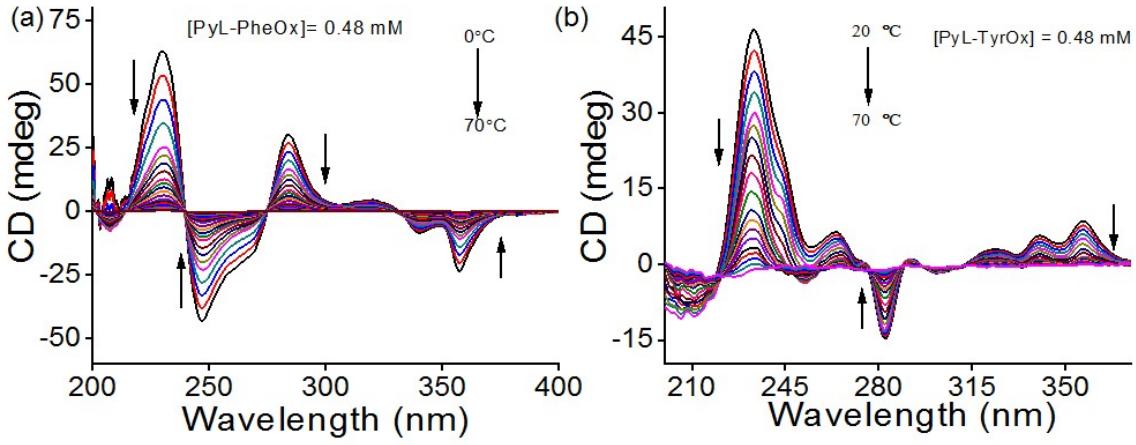

Figure S7. Variable temperature CD spectra of (a) **PyL-PheOx** (0.48 mM) and (b) **PyL-TyrOx** (0.48 mM) in water.

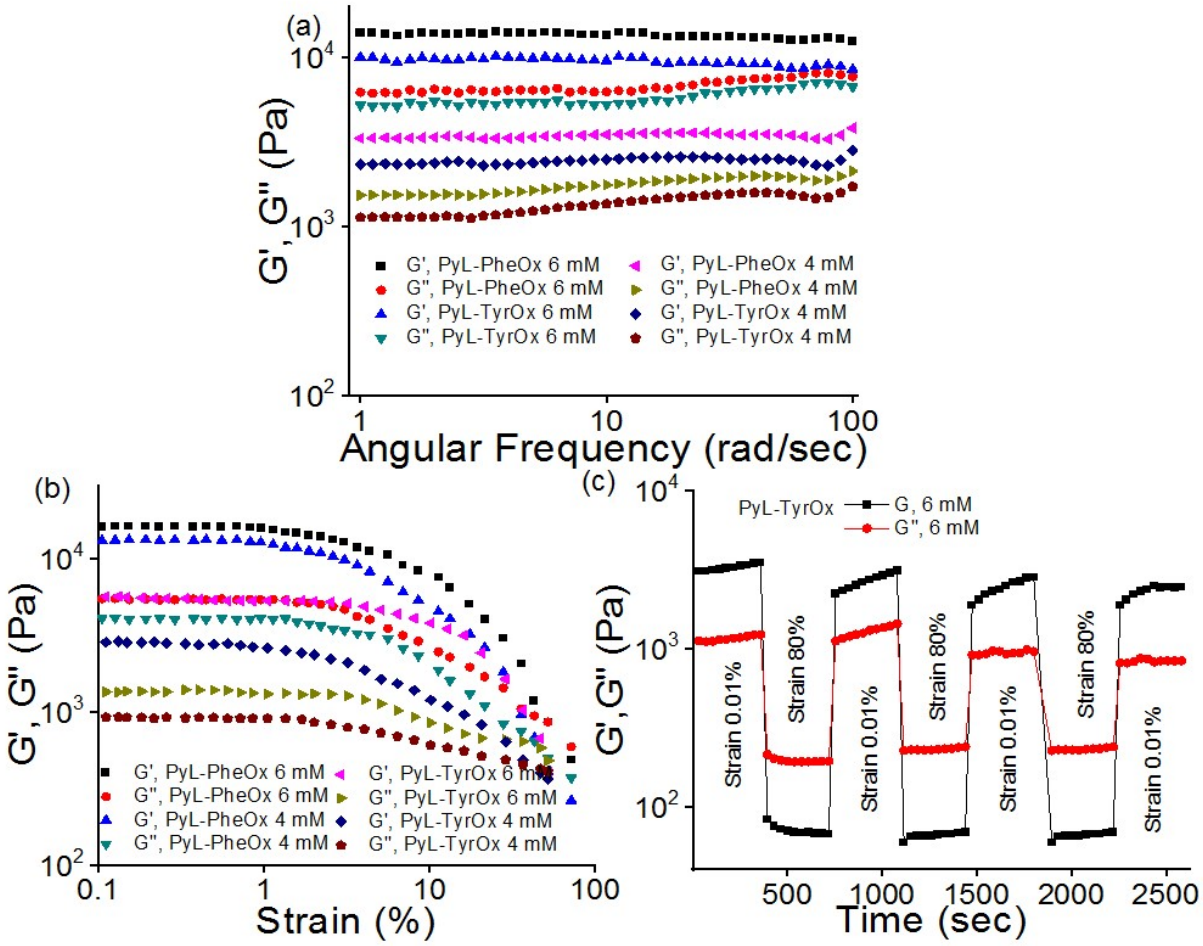

Figure S8. Variable concentration oscillatory (a) Frequency, (b) amplitude sweep rheology data of hydrogel of **PyL-PheOx** and **PyL-TyrOx**. (c) Hysteresis loop test of hydrogel of **PyL-TyrOx** (6 mM).

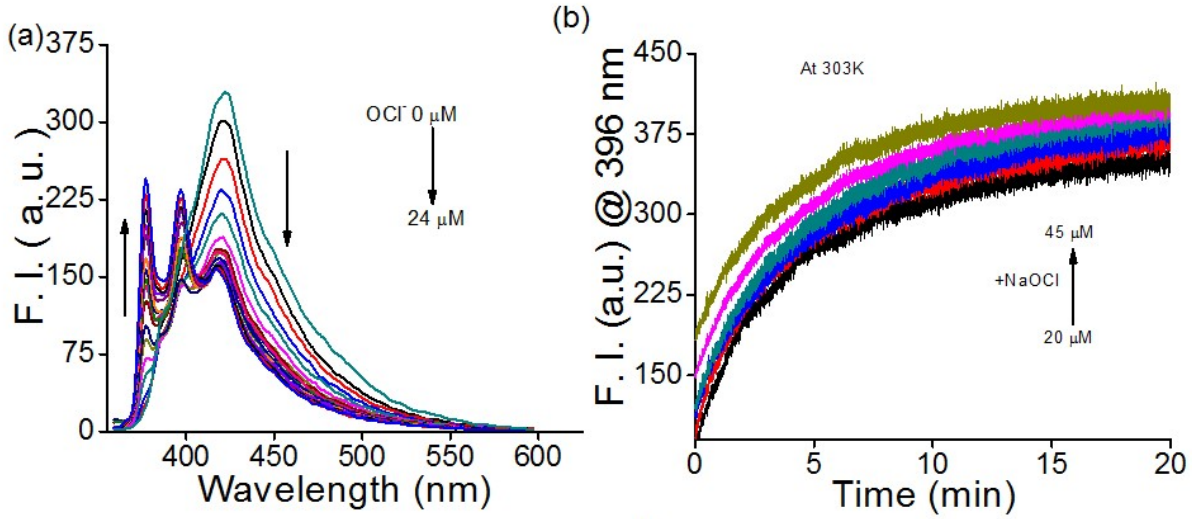

(c)

PyL-PheOx + ClO^- in μM	Rate (sec^{-1})
20	2.94
25	3.04
30	3.14
35	3.53
40	3.76
45	3.81

(d)

PyL-TyrOx + ClO^- in μM	Rate (sec^{-1})
20	5.46
25	8.64
30	9.00
35	9.06
40	9.78
45	9.84

Figure S9. (a) Fluorescence titration of **PyL-PheOx** (λ_{ex} = 345 nm, 20 μM), on interaction with ClO^-. (b) Kinetic studies of **PyL-PheOx** (λ_{ex} = 345 nm, 20 μM) on interaction with different concentration of ClO^- at 303K. Rate constant calculation of (c) **PyL-PheOx** (20 μM) and (d) **PyL-TyrOx** (20 μM) on interaction with different concentration of ClO^- at 303K.

(a)

Temperature (K)	Rate (sec^{-1})
293	3.48
303	5.46
313	9.42
323	28.2

(b)

Temperature (K)	Rate (sec^{-1})
293	2.54
303	3.26
313	17.06
323	19.46

Figure S10. Rate constant calculation of (a) **PyL-TyrOx** (20 μM) and (b) **PyL-PheOx** (20 μM) on interaction with ClO^- (20 μM) at different temperature.

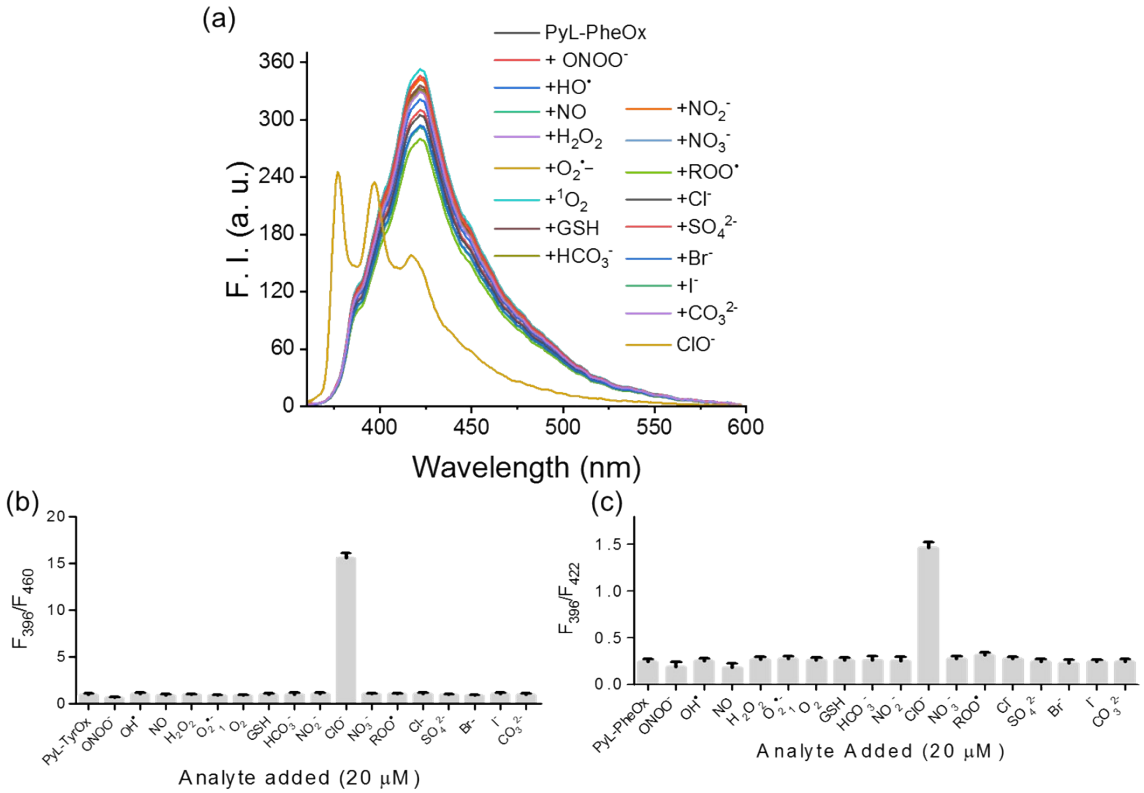

Figure S11. (a) Change in the emission spectra of **PyL-TyrOx** (20 μM, λ_{ex} = 345 nm) upon addition of various reactive oxygen species (20 μM). Plot showing the change in the emission spectra of (b) **PyL-TyrOx** (20 μM, λ_{ex} = 345 nm), (c) **PyL-PheOx** (20 μM, λ_{ex} = 345 nm) upon addition of various reactive oxygen species (20 μM).

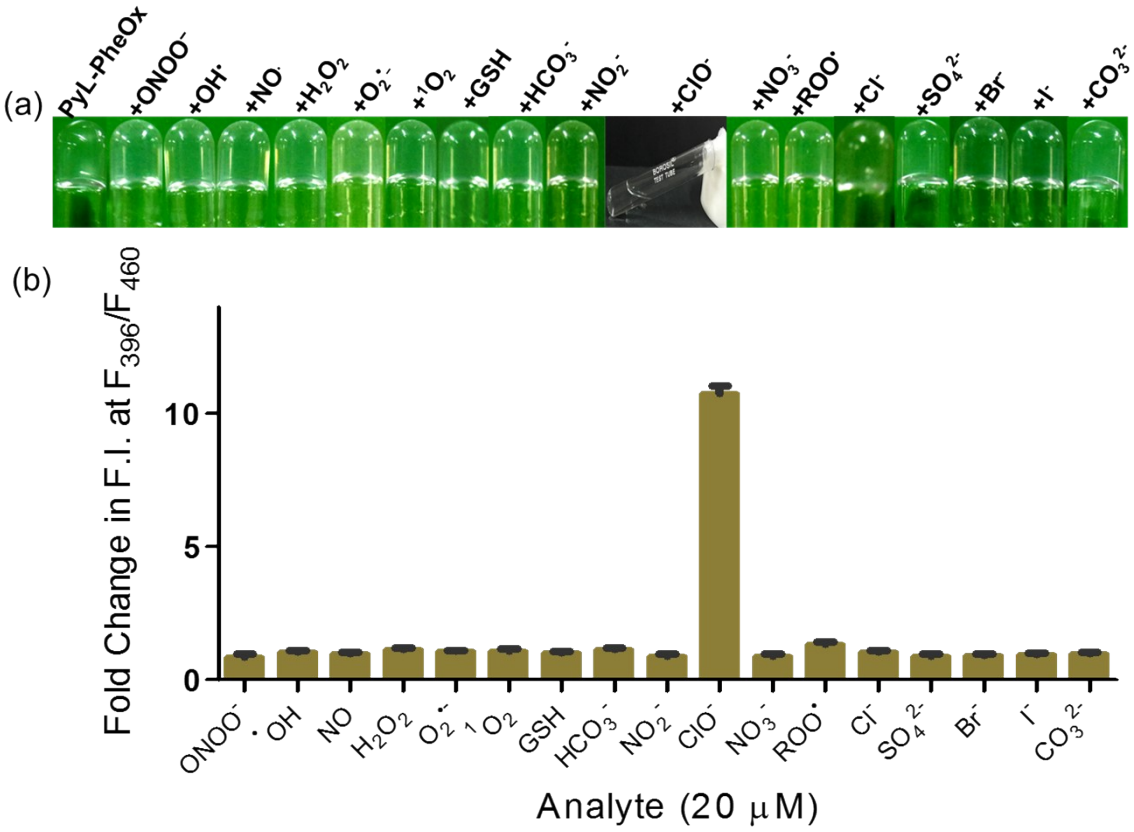

Figure S12: (a) Photographs of inverted tubes containing gel picture of **PyL-PheOx** (2.5 mM) in the presence of different ROS (1 mM). (b) Comparison of different analytes (20 μM) towards the interaction with **PyL-TyrOx** (20 μM, λ_{ex} = 345 nm) and its specific responses.

Sl. No	LOD (ppm)	Solvent	Response Time (min)	Application for detection of ClO^-	References
1	0.08	$CH_3CN–H_2O$ solution (4:6 v/v)	1	Tap water and TLC plates	*Dalton Trans.*, 2013, **42**, 10097-10101
2	0.008, 0.0017	PBS buffer (pH 7.4) with 0.1% DMSO	30	In vivo imaging in HeLa cells and in living mice	*Chem. Commun.*, 2014, **50**, 8640-8643
3	0.03	PBS buffer (pH 7.4) with 20% CH_3CN	5	Imaging in HepG2 cells	Chem. Commun., 2015, **51**, 10435-10438
4	0.02	Water solution (1% EtOH)	0.7	Imaging in RAW264.7 cells, P. aeruginosa and zebrafish	*Anal. Chim. Acta*, 2021, **1161**, 338472
5	0.002	HEPES buffer solution at pH 7.4	0.5	Tap Water and Imaging in HeLa cells	*Faraday Discuss*, 2017, **196**, 427-438
6	0.002	$Na_2B_4O_7$/NaOH buffer (pH 12) with 30% THF(v/v)	30	N/A	*Chem.-Eur. J.*, 2008, **14**, 4719-4724
7	0.05	PBS buffer (pH 7.4)	N/A	Imaging in tumors of living mice	*Anal. Chem.*, 2017, **89**, 5693-5696
8	0.0001	HEPES buffer solution at pH 7.4	3	Tap water and for Imaging in HeLa cells.	*Anal. Chem.,* 2014, **86**, 6315−6322
9	0.04	**PyL-TyrOx**	20	Commercial Bleach, Tap water, Pool water, Sea water, On site detection using pre-coated filter paper, gel-to-sol transition, Imaging in HeLa Cells	Present Work[a]

Table S1: A comparative literature survey on various hypochlorite sensors ([a]To best of our knowledge, this is the first report where a gel coated filter-paper based hydrogel system is developed for hypochlorite sensing via chemodosimetric interaction).

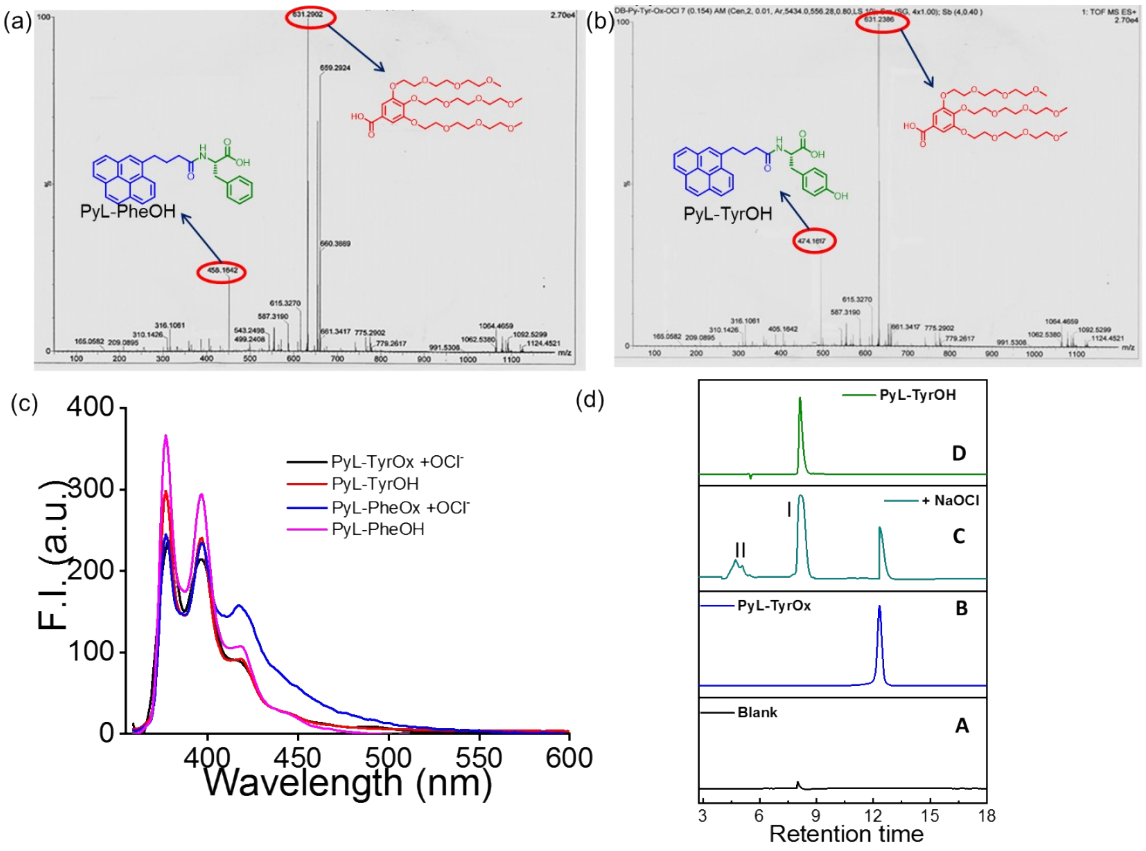

Figure S13. ESI-Mass spectra for the dissociative mechanism of (a) **PyL-PheOx** and (b) **PyL-TyrOx** on interaction with ClO^-. (c) Comparison emission spectra (λ_{ex} = 345 nm) of **PyL-PheOH** (20 μM) and **PyL-TyrOH** (20 μM) with **PyL-TyrOx** (20 μM) and **PyL-PheOx** (20 μM) in presence of ClO^- (20 μM). (d) HPLC traces of (A) Blank; (B) **PyL-TyrOx** (50 μM), (C) reaction of **PyL-TyrOx** (50 μM) with NaOCl (50 μM) and (D) **PyL-TyrOH** (50 μM). Reversed phase HPLC was performed on Sephadex GP-C18 column, 5μm, 150 mm × 4.6 mm with gradient elution using THF-water 3:7 mixture as the mobile phase. The formation of peaks was monitored at λ = 285 nm.

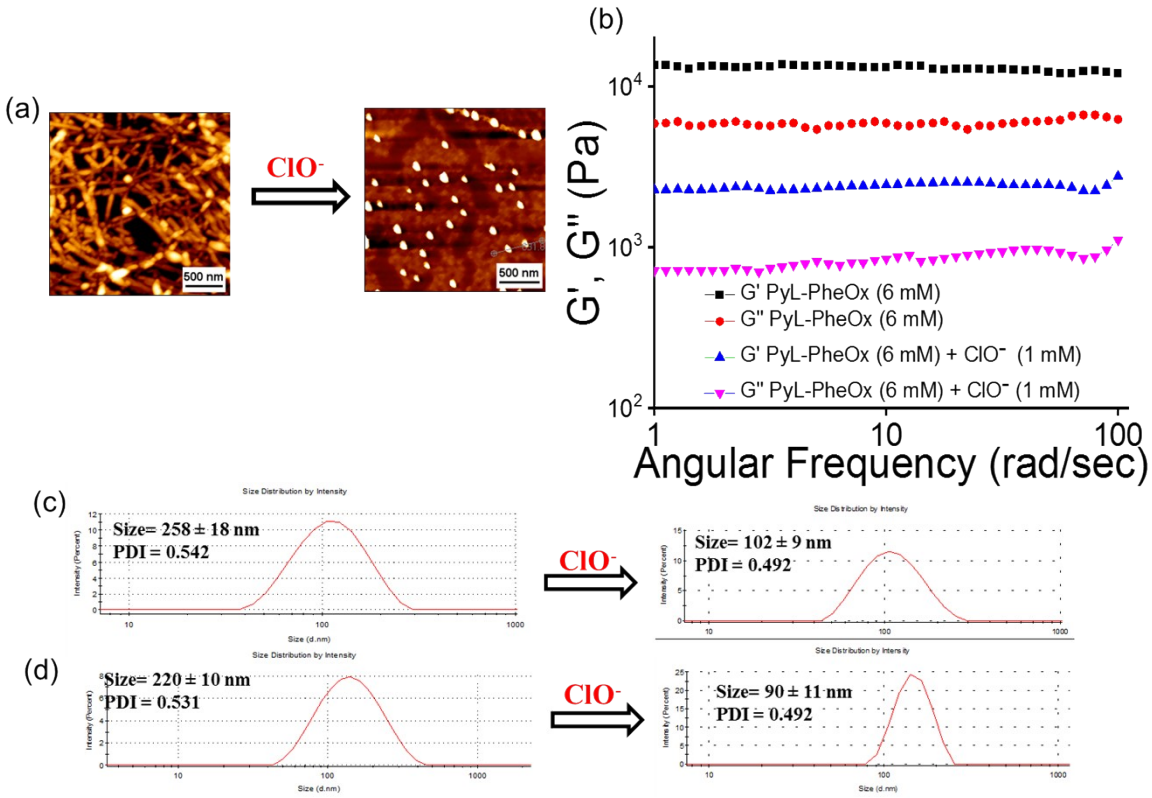

Figure S14. AFM images of **PyL-PheOx** in the presence of ClO^-. (b) Frequency sweep rheology data of **PyL-PheOx** in the presence of ClO^-. DLS data of (c) **PyL-PheOx** and (d) **PyL-TyrOx** in the presence of ClO^-.

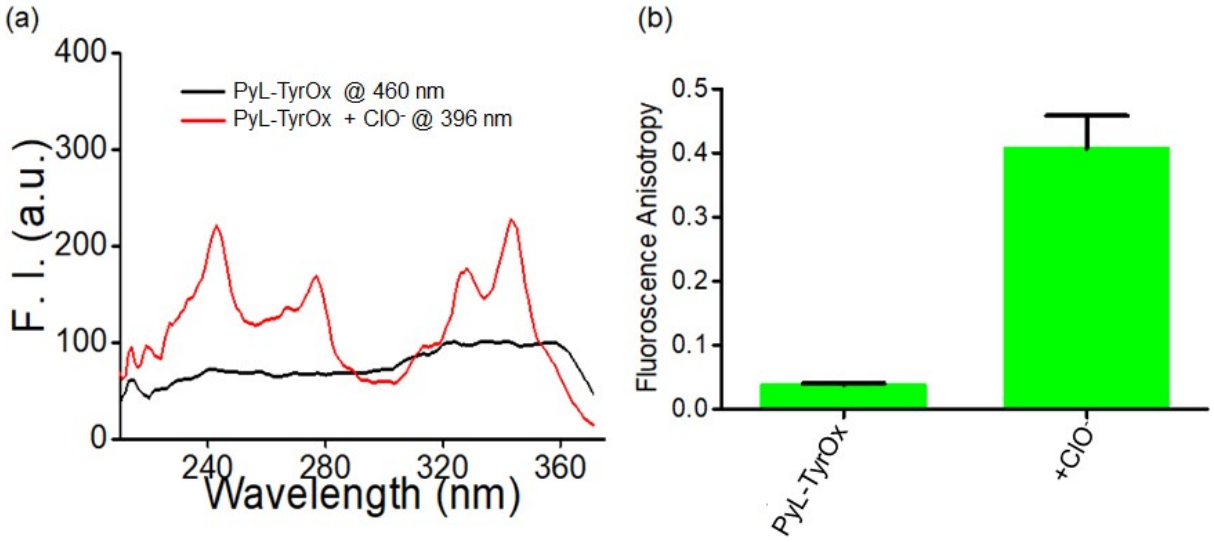

Figure S15. (a) Excitation spectra of **PyL-TyrOx** in the presence and absence of ClO^- in water. (b) Fluorescence anisotropy of **PyL-TyrOx** in the presence and absence of ClO^- in water at 460 nm.

(a)

ClO^- added (μM)	ClO^- calculated			ClO^- found	Recovery	RSD (%)
0	0	0	0	0	0	0
2	2.02	2.08	2.10	2.07	103.38	2.01
4	4. 16	4.32	4.01	4.16	104.08	3.72
6	6.18	6.09	6.29	6.19	103.16	1.62
8	8.12	8.02	8.25	8.13	101.63	1.42
10	10.04	10.19	10.28	10.17	101.70	1.19

(b)

ClO^-added (μM)	ClO^- calculated			ClO^- found	Recovery	RSD (%)
0	0	0	0	0	0	0
2	2.11	2.07	2.02	2.07	103.33	2.18
4	4.16	4.02	4.35	4.18	104.41	3.97
6	6.23	6.05	6.33	6.20	103.39	2.29
8	8.01	8.22	8.39	8.21	102.58	2.32
10	10.25	10.11	10.35	10.24	102.36	1.18

(c)

ClO^- added (μM)	ClO^- calculated			ClO^- found	Recovery	RSD (%)
0	0	0	0	0	0	0
2	2.12	2.10	2.05	2.09	104.50	1.73
4	4.06	4.22	4.11	4.13	103.25	1.98
6	6.11	6.02	6.09	6.07	101.16	0.78
8	8.23	8.09	8.15	8.16	102.00	0.86
10	10.14	10.04	10.31	10.16	101.6	1.34

Table S2. Estimation of ClO^- by **PyL-TyrOx** (20 μM, λ_{ex} = 345 nm), in (a) tap water, (b) Pool water and (c) Sea water sample.

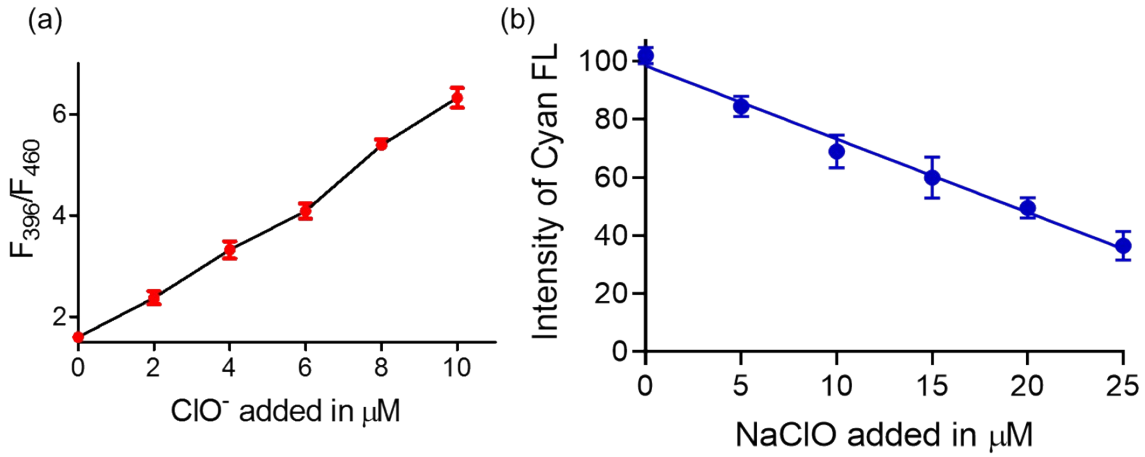

Figure S16. (a) Estimation of ClO^- in commercial bleach using **PyL-TyrOx** (20 μM, λ_{ex} = 345 nm). (b) Quantification of change in emission color of the hydrogel-coated paper strips upon gradual addition of ClO^- using image J.

Added [ClO^-] (μM)	Estimated [ClO^-] (μM)			Average value (μM)	Recovery (%)	Sample standard deviation	Relative standard deviation (%)
	Exp-1	Exp-2	Exp-3				
2	1.96	2.03	2.08	2.02	101.0	0.06	3
4	4.07	3.95	3.90	3.97	99.3	0.08	2.2
6	6.10	6.06	5.94	6.03	99.5	0.08	1.4
8	8.05	8.12	7.90	8.02	100.3	0.11	1.4
10	9.92	10.12	10.21	10.08	99.2	0.15	1.5

Table S3. Estimation of ClO^- by **PyL-TyrOx** (20 μM, λ_{ex} = 345 nm), in diluted bleach solution.

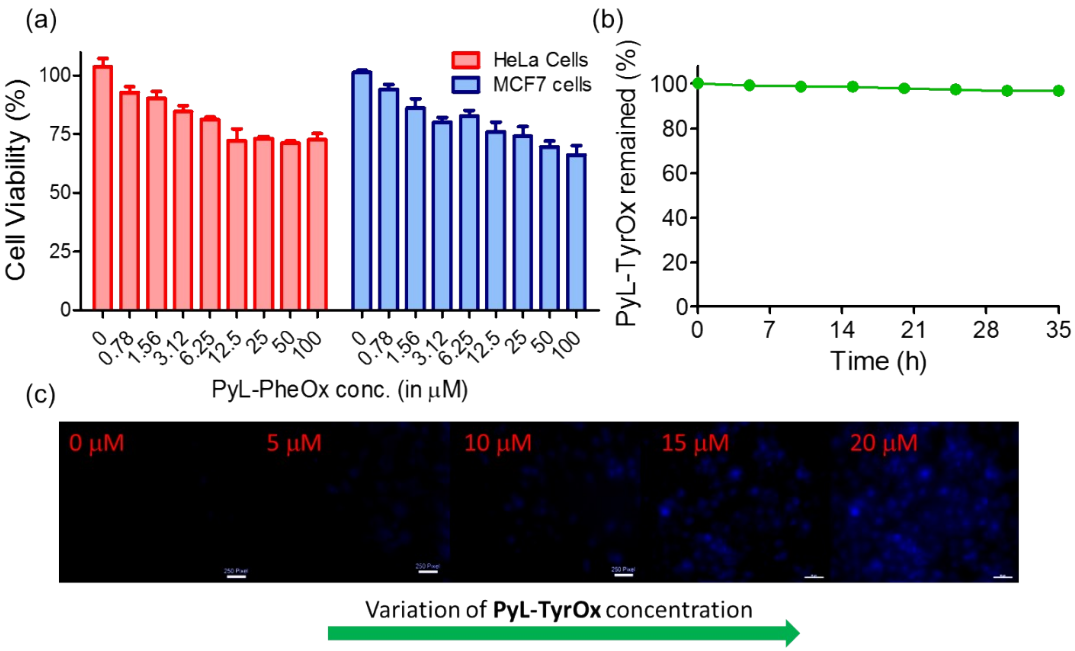

Figure S17. (a) MTT assay of **PyL-PheOx** (10 μM) in HeLa and MCF7 cell lines. (b) Time dependent proteolytic stability studies of **PyL-TyrOx** upon treatment of proteinase K (5 mg/mL) measured via ESI-MS mass spectrometry at physiological temperature (37 °C) and pH 7.4. (c) Effect of concentration of **PyL-TyrOx** (0-20 μM) on intracellular imaging using HeLa cells as model system after incubation over 20 min (at 37 °C).

References:

Sa. J. Nanda, A. Biswas and A. Banerjee, *Soft Matter*, 2013, **9**, 4198-4208

Sb. S. Bhattacharjee, B. Maiti and S. Bhattacharya, *Nanoscale*, 2016, **8**, 11224-11233.